Experimental Evaluation of Proposed Small-Molecule Inhibitors of Water Channel Aquaporin-1

Cristina Esteva-Font, Byung-Ju Jin, Sujin Lee, Puay-Wah Phuan, Marc O. Anderson, and A. S. Verkman

Departments of Medicine and Physiology, University of California, San Francisco, California (C.E.-F., B.-J.J., S.L., P.-W.P., A.S.V.); Department of Chemistry and Biochemistry, San Francisco State University, San Francisco, California (M.O.A.)

ABSTRACT

The aquaporin-1 (AQP1) water channel is a potentially important drug target, as AQP1 inhibition is predicted to have therapeutic action in edema, tumor growth, glaucoma, and other conditions. Here, we measured the AQP1 inhibition efficacy of 12 putative small-molecule AQP1 inhibitors reported in six recent studies, and one AQP1 activator. Osmotic water permeability was measured by stopped-flow light scattering in human and rat erythrocytes that natively express AQP1, in hemoglobin-free membrane vesicles from rat and human erythrocytes, and in plasma membrane vesicles isolated from AQP1-transfected Chinese hamster ovary cell cultures. As a positive control, 0.3 mM HgCl$_2$ inhibited AQP1 water permeability by >95%. We found that none of the tested compounds at 50 μM significantly inhibited or increased AQP1 water permeability in these assays. Identification of AQP1 inhibitors remains an important priority.

Introduction

The aquaporins (AQPs) are a family of small, plasma membrane proteins that transport water and/or small polar solutes such as glycerol (Carbrey and Agre, 2009; Verkman, 2012). The AQPs are a potentially important class of targets for drug development (Jeyaseelan et al., 2006; Wang et al., 2006; Frigeri et al., 2007; Verkman et al., 2014; Beitz et al., 2015), though there has been limited progress to date on the discovery and validation of AQP inhibitors. Challenges in the identification of AQP inhibitors include difficulties in assaying water permeability and the structural features of the AQPs, which include a narrow pore that excludes small molecules.

Aquaporin-1 (AQP1), originally identified as responsible for high water permeability in erythrocytes (Preston and Agre, 1991), is a particularly compelling drug target. In addition to erythrocytes, AQP1 is expressed in various fluid secreting and absorbing epithelia in kidneys, gastrointestinal organs, the central nervous system, the eye, and others as well in most microvascular endothelia including tumor microvessels (Hasegawa et al., 1994a; Nielsen et al., 1995; Mobasheri and Marples, 2004). Data largely from AQP1 knockout mice has suggested the potential utility of AQP1 inhibitors in the treatment of edema (Schnermann et al., 1998), tumors (Saadoun et al., 2005; Esteva-Font et al., 2014), and glaucoma (Zhang et al., 2002), and potentially for brain swelling (Oshio et al., 2005) and other conditions.

High-resolution structural data show that AQP1 monomers consist of six transmembrane helical segments and two partially spanning segments that surround a central aqueous pore (de Groot et al., 2001; Sui et al., 2001). AQP1 monomers further assemble in membranes as homotetramers (Verbavatz et al., 1993). Molecular dynamics modeling supports the conclusion that the single-file passage of water through the central pore of an AQP1 monomer, as well as interactions with residues lining the pore, is responsible for AQP1 water selectivity (Hub and de Groot, 2008). The narrowest section of the pore, named the ar/R constriction, consists of aromatic and arginine residues and has a diameter of 2.8 Å (Sui et al., 2001). The AQP1 pore excludes passage of small molecules and even protons, with the latter related to lack of stabilization of hydronium and/or geometric constraints (Gonen and Walz, 2006; Kato et al., 2006).

Heavy-metal, sulfhydryl-reactive small molecules such as HgCl$_2$ inhibit AQP1 water permeability by interaction with residue cysteine 187 near the extracellular surface of the AQP1 aqueous pore (Preston et al., 1993; Zhang et al., 1993). However, because of their lack of selectivity and toxicity, heavy metals are not drug development candidates.

ABBREVIATIONS: AqB013, 3-butylamino-4-phenoxy-*N*-pyridin-4-yl-5-sulfamoyl-benzamide; AqF026, 4-chloro-2-[(2-furanylmethyl) amino]-5-[[(phenylmethyl) amino] sulfonyl]-benzoic acid methyl ester; AQP, aquaporin; CHO, Chinese hamster ovary; DMSO, dimethylsulfoxide; HTS, high-throughput screening; NSC164914, tributyl-(2,4,5-trichlorophenoxy) stannane; NSC168597, tributyl lead chloride; NSC301460, trichopolyn I; NSC657298, (*E*)-1-[1-ethyl-4-hydroxy-4-[(*E*)-2-(4-methylphenyl) ethenyl] piperidin-3-yl]-3-(4-methylphenyl) prop-2-en-1-one; NSC670226, 2-[4-tert-butyl-1-[(4-fluorophenyl) methyl] cyclohexyl] oxy-*N*,*N*-dimethylethanamine; NSC670229, 2-[4-tert-butyl-1-[(4-methylphenyl) methyl] cyclohexyl] oxy-*N*,*N*-dimethylethanamine; PBS, phosphate-buffered saline.

Early studies reported AQP1 inhibition by carbonic anhydrase inhibitors such as acetazolamide and K$^+$ channel blockers such as tetraethylammonium (Brooks et al., 2000; Detmers et al., 2006), though subsequent reevaluation using different assays did not confirm AQP1 water transport inhibition by these molecules (Yang et al., 2006, 2008; Søgaard and Zeuthen, 2008; Yamaguchi et al., 2012). More recently, a variety of approaches, including high-throughput screening and computational chemistry, have yielded compounds with reported AQP1 inhibition or activation activity (Migliati et al., 2009; Mola et al., 2009; Seeliger et al., 2013; Yool et al., 2013; To et al., 2015; Patil et al., 2016), as summarized in Fig. 1 and Table 1. Motivated by the high potential clinical utility of small-molecule AQP1 inhibitors, here we tested these various proposed AQP1 inhibitors, comparing their water transport inhibition activity in different cellular systems with that of HgCl$_2$.

Materials and Methods

Compounds. Compounds 1 [1,3-phenylenediacrylic acid], 2 [(E,Z)-3-methyl-4-(2-quinolinylmethylene)-2-pentenedioic acid disodium salt], and 3 [N-(1,3-benzodioxol-5-ylmethyl)-N′-2,1,3-benzothiadiazol-5-yl-thiourea] were purchased from ChemBridge (San Diego, CA). Compounds 6 (NSC168597 [tributyl lead chloride]), 7 (NSC301460 [trichopolyn I]), 8 (NSC164914 [tributyl-(2,4,5-trichlorophenoxy) stannane]), 9 (NSC670229 [2-[4-tert-butyl-1-[(4-methylphenyl) methyl] cyclohexyl] oxy-N,N-dimethylethanamine]), 10 (NSC670226 [2-[4-tert-butyl-1-[(4-fluorophenyl) methyl] cyclohexyl] oxy-N,N-dimethylethanamine]), and 11 (NSC657298 [(E)-1-[1-ethyl-4-hydroxy-4-[(E)-2-(4-methylphenyl) ethenyl] piperidin-3-yl]-3-(4-methylphenyl) prop-2-en-1-one]) were purchased from the National Cancer Institute. Compound 13 [N-[[trans-4-[[(4-amino-2-quinazolinyl) amino] methyl] cyclohexyl] methyl]-1-naphthalenesulfonamide] was purchased from Tocris

Biosciences (Denver, CO). All other chemicals were purchased from Sigma-Aldrich (St. Louis, MO). Compounds 4 (AqB013 [3-butylamino-4-phenoxy-N-pyridin-4-yl-5-sulfamoyl-benzamide]), 5 (AqF026 [4-chloro-2-[(2-furanylmethyl) amino]-5-[[(phenylmethyl) amino] sulfonyl]-benzoic acid methyl ester]), and 12 [1-(7-(2,4-dichlorophenyl)-5-fluoro-2,3-dihydrobenzofuran-2-yl)-N-methylmethanamine] were synthesized. Compound 5 (AqF026) was synthesized from furosemide as reported (Yool et al., 2013), and the analytic data matched with the reported data.

Compound 4 (AqB013) was synthesized from bumetanide through an imidazolide intermediate (Migliati et al., 2009). To a suspension of bumetanide (100 mg, 0.27 mmol) in ethyl acetate (1 mL) was added 1,1′-carbonyldiimidazole (50 mg, 0.3 mmol) under N$_2$. The mixture was heated for 1 hour and cooled to room temperature. The resulting precipitate was filtered and washed with ethyl acetate and dried in vacuo to give intermediate 3-(butylamino)-5-(1H-imidazole-1-carbonyl)-2-phenoxybenzenesulfonamide as a white solid (105 mg, 90%). To this compound (10 mg, 0.024 mmol) in tetrahydrofuran (1 mL) was added 4-aminopyridine (4 mg, 0.042 mmol) and trifluoroacetic acid (catalytic amount) and stirred overnight. The reaction mixture was evaporated under reduced pressure. Compound 4 was obtained as a yellowish white solid (6 mg, 56%) after silica gel column chromatography. ^{1}H-NMR (300 MHz, CD$_3$OD): δ 8.19 (brs, 1H), 7.62 (m, 2H), 7.35–7.29 (m, 2H), 7.26 (d, 1H, J = 2.0 Hz), 7.15–7.13 (m, 1H), 7.08 (t, 1H, J = 6.3 Hz), 6.95 (d, 2H, J = 7.7 Hz), 3.08 (t, 2H, J = 6.9 Hz), 1.46–1.36 (m, 2H), 1.17–1.09 (m, 2H), 0.79 (t, 2H, J = 7.3 Hz); liquid chromatography with mass spectrometry (electrospray ionization): 441 (M+H)$^+$.

Compound 12 was synthesized by Suzuki coupling of (7-bromo-5-fluoro-2,3-dihydrobenzofuran-2-yl)methyl-4-methylbenzenesulfonate and 2,4-dichlorophenylboronic acid under microwave irradiation, followed by alkylation with methyl amine at 60°C in dimethylsulfoxide (DMSO) overnight. ^{1}H-NMR (300 MHz, CD$_3$OD): δ 7.56 (dd, 1H, J = 1.7, 0.6 Hz), 7.39–7.37 (m, 2H), 7.05–7.02 (m, 1H), 6.80 (dd, 1H, J = 9.5, 2.7 Hz), 4.99–4.96 (m, 1H), 3.42 (m, 1H), 3.06–2.83 (m, 3H), 2.45 (s, 3H); ^{13}C-NMR (75 MHz, CD$_3$OD): δ 153.0, 152.4, 134.3, 133.8, 132.4, 128.9, 128.8, 126.8, 120.4, 120.3, 116.1, 114.7, 112.1, 81.9, 54.8, 34.4,
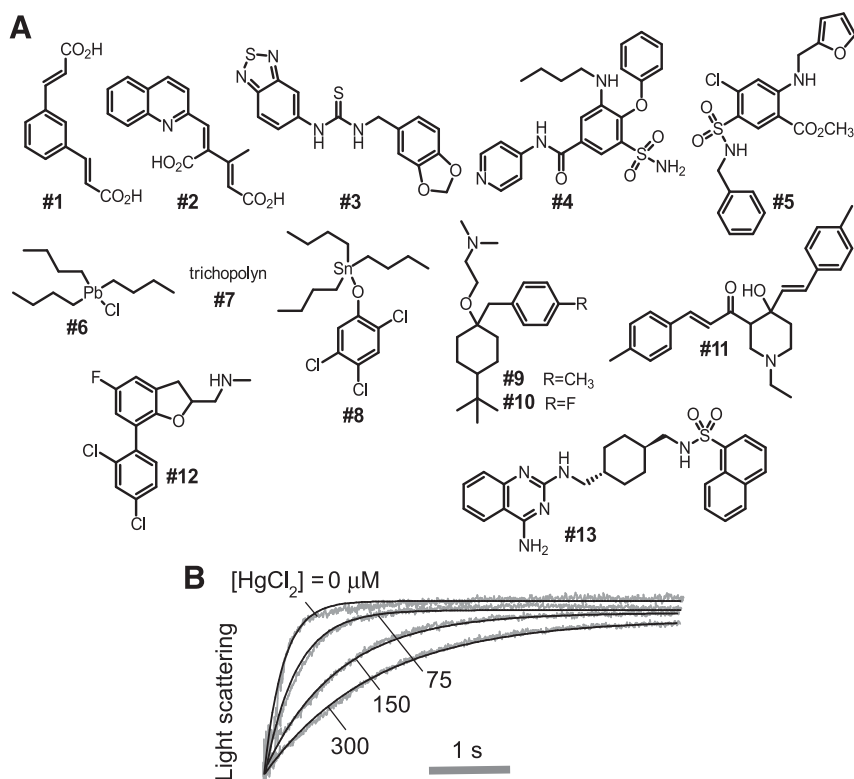
Fig. 1. Chemical structures of putative AQP1 inhibitors. (A) Structures of inhibitors reported by Migliati et al. (2009), Mola et al. (2009), Yool et al. (2013), Seeliger et al. (2013), To et al. (2015), and Patil et al. (2016) (see Table 1). (B) Osmotic water permeability in human erythrocytes as measured from the time course of scattered light intensity in response to a 250 mM inwardly directed sucrose gradient at room temperature. Erythrocytes were incubated with 0, 75, 150, or 300 μM HgCl$_2$ for 5 minutes before measurement.

TABLE 1
Reported small-molecule AQP1 modulators

Compound		Reference	Identification Method	Reported IC$_{50}$ (μM)
Code	Name			
Inhibitor				
Compound 1	1,3-Phenylenediacrylic acid	Seeliger et al., 2013	*Xenopus laevis* oocytes	8
Compound 2	(*E*,*Z*)-3-methyl-4-(2-quinolinylmethylene)-2-pentenedioic acid disodium salt	Seeliger et al., 2013	*Xenopus laevis* oocytes	17
Compound 3	*N*-(1,3-benzodioxol-5-ylmethyl)-*N*′-2,1,3-benzothiadiazol-5-yl-thiourea	Seeliger et al., 2013	*Xenopus laevis* oocytes	18
AqB013 (Compound 4)	3-Butylamino-4-phenoxy-*N*-pyridin-4-yl-5-sulfamoyl-benzamide	Migliati et al., 2009	Virtual screen, *Xenopus laevis* oocytes	20
NSC168597 (Compound 6)	Tributyl lead chloride	Mola et al., 2009	Calcein cell-based assay	49
NSC301460 (Compound 7)	Trichopolyn I	Mola et al., 2009	Calcein cell-based assay	28
NSC164914 (Compound 8)	Tributyl-(2,4,5-trichlorophenoxy) stannane	Mola et al., 2009	Calcein cell-based assay	40
NSC670229 (Compound 9)	2-[4-Tert-butyl-1-[(4-methylphenyl) methyl] cyclohexyl] oxy-*N*,*N*-dimethylethanamine	Mola et al., 2009	Calcein cell-based assay	27
NSC670226 (Compound 10)	2-[4-Tert-butyl-1-[(4-fluorophenyl) methyl] cyclohexyl] oxy-*N*,*N*-dimethylethanamine	To et al., 2015	Yeast freeze-thaw assay	20
NSC657298 (Compound 11)	(*E*)-1-[1-ethyl-4-hydroxy-4-[(*E*)-2-(4-methylphenyl) ethenyl] piperidin-3-yl]-3-(4-methylphenyl) prop-2-en-1-one	To et al., 2015	Yeast freeze-thaw assay	48
Compound 12	1-(7-(2,4-Dichlorophenyl)-5-fluoro-2,3-dihydrobenzofuran-2-yl)-*N*-methylmethanamine	Patil et al., 2016	Calcein cell-based assay	10
Compound 13	*N*-[[trans-4-[[(4-amino-2-quinazolinyl) amino] methyl] cyclohexyl] methyl]-1-naphthalenesulfonamide	Patil et al., 2016	Calcein cell-based assay	3
Activator				Reported EC$_{50}$ (μM)
AqF026 (Compound 5)	4-Chloro-2-[(2-furanylmethyl) amino]-5-[[(phenylmethyl) amino] sulfonyl]-benzoic acid methyl ester	Yool et al., 2013	Virtual screen, *Xenopus laevis* oocytes	3.3

33.2; liquid chromatography with mass spectrometry (electrospray ionization): 326 (M+H)$^+$.

Collection of Human and Rat Blood. Human venous blood obtained from a single donor was collected into K3EDTA Vacutainers (Greiner, Kremsmunster, Austria). Whole rat blood was collected from adult Wistar rats (250–300 g) purchased from Charles River Laboratories (Wilmington, MA) by cardiac puncture under isoflurane anesthesia. Animal protocols were approved by the University of California, San Francisco Committee on Animal Research.

Preparation of Hemoglobin-Free Erythrocyte Ghosts. Ghost membranes were prepared by the procedure of Zeidel et al. (1992), with modifications. Collected blood was washed 3 times with phosphate-buffered saline (PBS) by centrifugation at 800g for 5 minutes at 4°C. The erythrocyte pellet was resuspended in 0.1x PBS (hypotonic buffer), and the membranes were washed twice in the same buffer by centrifugation at 30,000g for 10 minutes at 4°C. Hypertonic (10x) PBS was added to restore isotonicity, and membranes were incubated for 1 hour at 37°C to allow resealing. The resulting ghost membrane vesicles were resuspended at ~0.4 mg protein/ml for stopped-flow measurements.

Erythrocyte Labeling. Erythrocytes were washed 3 times with PBS (3000g, 15 minutes) and then fluorescently labeled by incubation with 15 μM calcein-AM (Invitrogen, Carlsbad, CA) at 37°C for 1.5 hours. Erythrocytes were then washed twice with PBS (3000g, 10 minutes) to remove extracellular dye and diluted 15-fold in PBS.

Cell Culture. Chinese hamster ovary (CHO) cells stably expressing human AQP1 or AQP4-M23, generated as reported (Ma et al., 1993, Phuan et al., 2012), and nontransfected CHO cells were grown in Ham's F-12 nutrient medium supplemented with 10% fetal bovine serum, 100 units/ml penicillin, and 100 μg/ml streptomycin. Geneticin (500 μg/ml) was used as a selection marker for the cells expressing AQP1 and AQP4-M23. Cells were grown at 37°C in 5% CO$_2$ and 95% air.

Preparation of Plasma Membrane Vesicles from CHO Cells. Enriched plasma membrane fractions were prepared as described elsewhere (Rossi et al., 2012). CHO cells from 10 confluent 175 cm^2 flasks (Thermo Scientific, Rochester, NY) were homogenized by 20 strokes of a glass Dounce homogenizer in 250 mM sucrose, 10 mM Tris-HCl, and 1 mM EDTA containing protease inhibitors (Complete Mini; Roche Diagnostics, Mannheim, Germany). The homogenate was then centrifuged at 4000g for 15 minutes at 4°C, and the enriched plasma membrane fraction was obtained by centrifugation at 17,000g for 45 minutes. The resultant pellet was suspended in PBS for stopped-flow measurements.

Stopped-Flow Measurements. Osmotic water permeability was measured by stopped-flow light scattering (or fluorescence) using a Hi-Tech Sf-51 instrument (Wiltshire, United Kingdom) as described by Jin et al. (2015). Intact erythrocytes (hematocrit ~0.5%), hemoglobin-free erythrocyte ghost membranes (~0.4 mg protein/ml), plasma membrane vesicles from CHO cells (~0.8 mg protein/ml), or calcein-labeled erythrocytes were suspended in PBS and subjected to a 250 mOsm inwardly directed gradient of sucrose. Some experiments were performed with a 150 mOsm outwardly directed NaCl gradient produced by mixing equal volumes of the membrane suspension in PBS with distilled water. The resultant kinetics of cell volume were measured from the time course of 90° scattered light intensity at 530 nm (or calcein fluorescence) in which increasing scattered light intensity corresponds to decreasing cell volume.

For the testing of putative AQP1 modulators, compounds in DMSO (0.5% final DMSO concentration) were incubated with cell or membrane suspensions for >10 minutes at 50 μM before stopped-flow measurement. Relative osmotic water permeability was determined by exponential regression using Prism software (GraphPad Software, San Diego, CA).

Erythrocyte Hemoglobin Release. Compounds (50 μM, 0.5% final DMSO concentration) were incubated with a freshly prepared

erythrocyte suspension for 15 minutes and centrifuged at 3000 rpm for 10 minutes. Hemoglobin released in the supernatant was measured by absorbance at 540 nm. In some studies, erythrocyte morphology was assessed by phase-contrast microscopy at $1000\times$ magnification.

Statistical Analysis. Data are presented as the mean standard error of the mean (S.E.M.) of at least four independent experiments, and were analyzed with paired Student's t test or one-way analysis of variance (ANOVA).

Results

Figure 1A shows chemical structures of the 12 putative AQP1 inhibitors and one AQP1 activator studied here. $HgCl_2$ was used as a positive control for inhibition. Figure 1B shows $HgCl_2$ concentration-dependent inhibition of water permeability in human erythrocytes, which natively express AQP1. Osmotic water permeability was measured by the established stopped-flow light-scattering method in which a dilute erythrocyte suspension was mixed rapidly with an anisosmolar solution to impose a 250 mM inwardly directed sucrose gradient. The sucrose gradient causes osmotic water efflux and cell shrinkage, seen as increasing scattered light intensity at 530 nm wavelength. The IC_{50} for $HgCl_2$ inhibition of erythrocyte AQP1 water permeability was ~85 μM.

Similar studies were performed for the putative AQP1 modulators at 50 μM, a concentration predicted from published data to strongly inhibit (or weakly activate) AQP1 water permeability (published IC_{50} values listed in Table 1). Compounds were incubated with the erythrocyte suspension for at least 15 minutes before stopped-flow measurements. Representative light-scattering curves are shown for human erythrocytes in Fig. 2A (left) with averaged data ($\pm$ S.E.M.) summarized in Fig. 2B (left). Whereas $HgCl_2$ strongly inhibited osmotic water permeability in human erythrocytes, no significant effect was seen for any of the 13 test compounds.

Reasoning that the lack of inhibition might be due to the presence of hemoglobin in the erythrocyte cytoplasm, which potentially could bind compounds, we performed similar studies in sealed, hemoglobin-free ghost membranes prepared from human erythrocytes. Similar to the results in Fig. 2A, no significant effect on osmotic water permeability by the test compounds was seen in ghost membranes, with $HgCl_2$ showing strong inhibition as positive control.

As it is possible, though unlikely, that inhibition efficacy could depend on the direction of water flow, compounds were also tested in human erythrocytes using a stopped-flow light-scattering assay of osmotic swelling in which cells were exposed to 50% hypotonic saline. Compounds 9, 10, and 13 showed apparent weak inhibition of water permeability (30%–40% at 50 μM) whereas the other compounds had no effect on water permeability (Fig. 3).

Because potential artifacts in light-scattering assays could be produced, for example, by erythrocyte crenation or aggregation, compounds were also tested using a calcein-quenching assay of osmotic swelling. This assay is based on volume-dependent calcein quenching, which is insensitive to factors such as cell shape that can affect light scattering. Figure 4 shows that none of the 13 compounds significantly affected erythrocyte water permeability. The reduced fluorescence signal intensity for compound 12 suggests partial erythrocyte lysis.
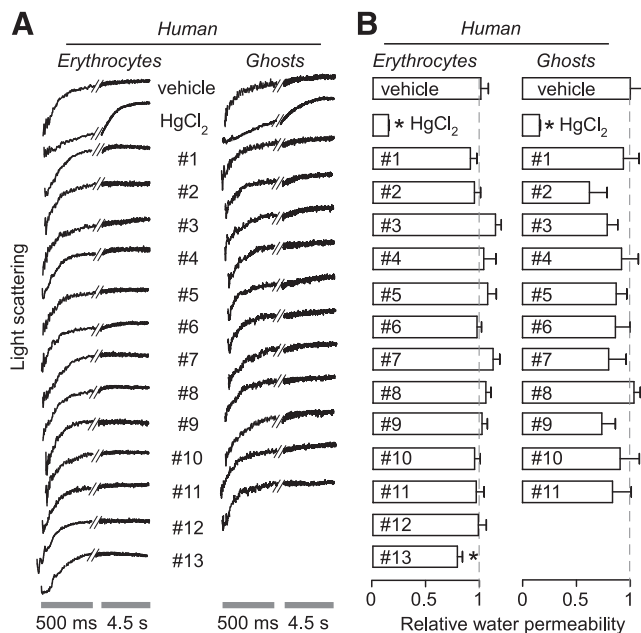
Fig. 2. Osmotic water permeability in human erythrocytes and hemoglobin-free ghost membranes derived therefrom. Osmotic water permeability was measured from the time course of scattered-light intensity in response to a 250 mM inwardly directed sucrose gradient. (A) Representative time course data for negative control (0.5% DMSO vehicle alone), 0.3 mM $HgCl_2$ (positive control), and indicated compounds (each 50 μM). Cells and ghosts were incubated with test compounds for 15 minutes before measurements. (B) Relative osmotic water permeability (S.E., $n = 4$). *$P < 0.05$ compared with control.

To investigate the possible reasons for the effects of compounds 9, 10, and 13 in the light-scattering assay of osmotic swelling, we evaluated erythrocyte toxicity by use of a hemoglobin-release assay and by cell morphology. Compounds 6 and 8 to 13 caused significantly greater hemoglobin release than the vehicle control. Direct examination of erythrocyte morphology at high magnification showed marked abnormalities for compounds 6, 9, 10, 12, and 13, with cell crenation and variable aggregation (Fig. 5B). These abnormalities may account for the apparent artifacts in the light-scattering assay of cell swelling.

Stopped-flow light-scattering measurements were also performed using rat erythrocytes, which express rat AQP1, and sealed, hemoglobin-free ghost membranes prepared from rat erythrocytes (Fig. 6). As found with human erythrocytes and ghost membranes, no significant effect on osmotic water permeability was seen for any of the test compounds, with $HgCl_2$ showing strong inhibition as positive control.

To test for AQP1 inhibition in a different cellular context, AQP1-enriched plasma membrane vesicles were isolated from AQP1-transfected (and control) CHO cells by homogenization and differential centrifugation. Osmotic water permeability was measured by stopped-flow light scattering as done for the erythrocytes and erythrocyte ghost membranes. Figure 7A shows that membrane vesicle shrinkage was ~5-fold more rapid in vesicles prepared from AQP1-transfected CHO cells than control (nontransfected) CHO cells. Osmotic water permeability was inhibited by ~85% by 0.3 mM $HgCl_2$.

As another control, plasma membrane vesicles were prepared from CHO cells expressing AQP4, a water-selective channel that was originally named MIWC (mercurial-insensitive
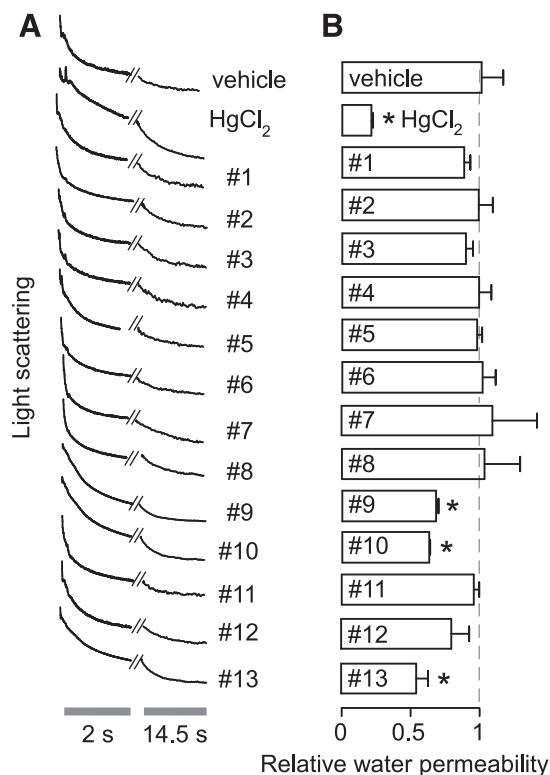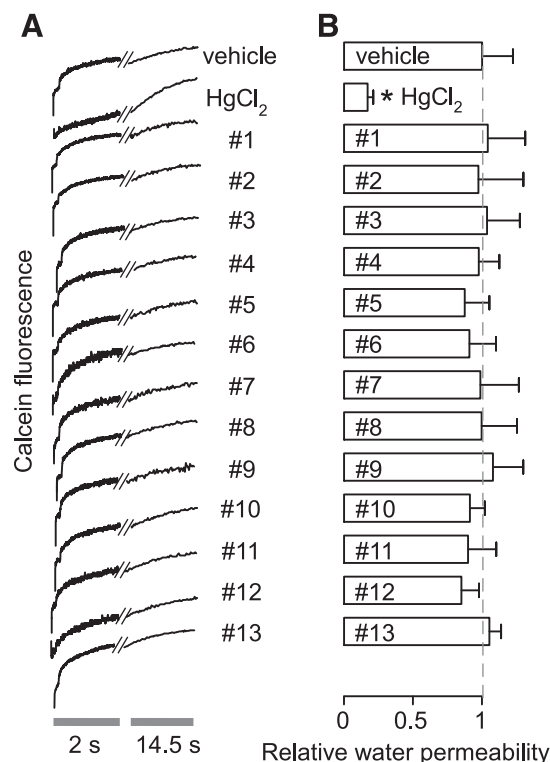
Fig. 3. Osmotic swelling of human erythrocytes. Osmotic water permeability was measured from the time course of scattered-light intensity in response to a 150 mOsm outwardly directed osmotic gradient. (A) Representative time course data for negative control (0.5% DMSO vehicle alone), 0.3 mM $HgCl_2$ (positive control), and indicated compounds (each 50 μM). (B) Relative osmotic water permeability (S.E., $n = 4$). *$P <$ 0.05 compared with negative control (0.5% DMSO vehicle alone). Cells and ghosts were incubated with test compounds for ~15 minutes before measurements.

Fig. 4. Osmotic swelling of calcein-labeled human erythrocytes. Osmotic water permeability was measured from the time course of intracellular calcein fluorescence in response to a 150 mOsm outwardly directed osmotic gradient. (A) Representative time course data for negative control (0.5% DMSO vehicle alone), 0.3 mM $HgCl_2$ (positive control), and indicated compounds (each 50 μM). (B) Relative osmotic water permeability (S.E., $n = 4$). *$P < 0.05$ compared with negative control (0.5% DMSO vehicle alone).

water channel) (Hasegawa et al., 1994b), whose water permeability is not inhibited by $HgCl_2$ because of absence of a critical cysteine residue (Shi and Verkman, 1996). Osmotic water permeability in the AQP4-containing membrane vesicles was ~5-fold more rapid than in control vesicles, and, in contrast to the AQP1-containing vesicles, it is not inhibited by $HgCl_2$.

Figure 7B shows representative light-scattering data and averaged results for measurements of osmotic water permeability in the AQP1-containing plasma membrane vesicles. No significant effect was found for any of the test compounds.

Discussion

We tested 12 putative AQP1 inhibitors and one putative activator for their efficacy in reducing or increasing osmotic water permeability in rat and human erythrocytes and ghost membranes, and plasma membrane vesicles from AQP1-transfected CHO cells. At 50 μM, a concentration well above reported IC_{50} values for each of the compounds, no significant water transport inhibition or activation was found using stopped-flow assays with sensitivity to detect as small as a 5%–10% change in water permeability. The well-studied, albeit nonselective AQP1 inhibitor $HgCl_2$ showed strong inhibition in all assay systems. The small apparent inhibition by compounds 9, 10, and 13 seen in the light-scattering swelling assay in human erythrocytes was likely an artifact,

as these compounds were found to cause cell crenation and aggregation, and inhibition was not seen in the calcein fluorescence quenching assay. We conclude that, other than nonselective, sulfhydryl-reactive, heavy metal-containing compounds, no confirmed small-molecule AQP1 inhibitors have been reported to date. Albeit a negative study, the work here underscores the need to test putative AQP inhibitors using robust, sensitive assays, and, given the major potential clinical applications of AQP1 inhibitors, the need for continued screening and computational work to identify useful inhibitors.

It is not known why AQP1 appears to be refractory to identification of small-molecule inhibitors. Part of the reason may be its unique structure, in which small, relatively rigid monomers containing water-only pores are assembled in membranes as homotetramers. The narrow AQP1 water pore excludes small molecules; even if a small molecule could bind to the vestibule adjacent to the pore, there may remain many paths for water flow around the small molecule, as if trying to cork a wine bottle with a randomly shaped stone. However, though direct pore blockade may be difficult to achieve, allosteric closure of the pore from a distant site would seem possible. Perhaps the tight, relatively rigid structure of the AQP1 monomer, as well as its narrow pore region and small extracellular footprint, resists allosteric pore closure by externally bound molecules. In unpublished work (M.O. Anderson, C. Esteva-Font, and A.S. Verkman) we did not identify any useful AQP1 inhibitors from a screen
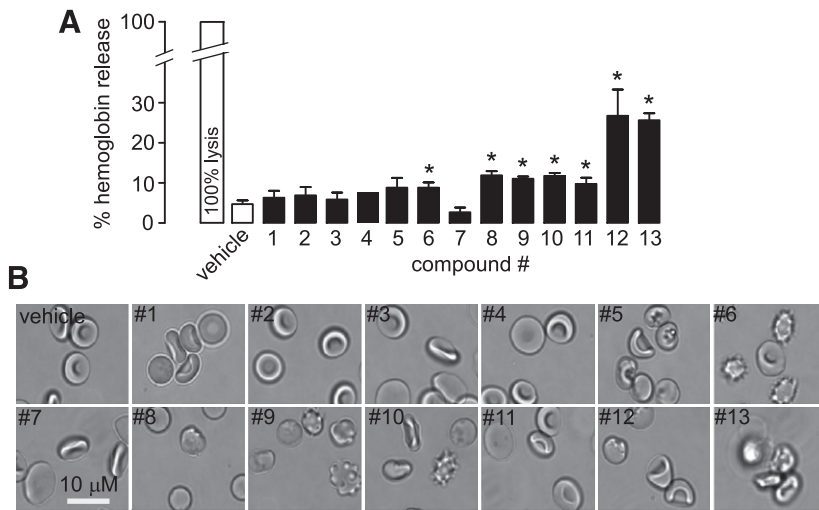
Fig. 5. Compound effects on hemoglobin release and erythrocyte morphology. (A) Hemoglobin release from human erythrocytes after 15 minutes of incubation with test compounds at 50 μM (S.E., $n = 4$). *$P < 0.05$ compared with control. (B) Representative phase-contrast photomicrographs of human erythrocytes after 15-minute incubations with test compounds.

of ~150,000 synthetic small molecules with an erythrocyte lysis assay that was used successfully to identify nanomolar-potency urea transport inhibitors (Levin et al., 2007). We also did not identify any useful AQP1 inhibitors in a computational docking study of 10^6 commercially available compounds, followed by a water transport assay of 2000 compounds with the highest docking scores.

It is also unclear why many putative AQP1 modulators have been reported in the literature, but water transport inhibition (or activation) cannot be confirmed, including the 13 small molecules studied here, and previously acetazolamide, tetraethylammonium, and dimethylsulfoxide (Yang et al., 2006; Tanimura et al., 2009). As discussed elsewhere (Verkman et al., 2014), part of the reason may be that the functional assays

largely relied on the *Xenopus oocyte* expression system and calcein-loaded cell cultures, both of which are subject to artifacts. For example, compounds that affect cell size or shape, cell volume regulation, nonaquaporin ion or solute transporters, or calcein fluorescence quenching could appear to inhibit water permeability in these systems. Inhibitors of cellular proteins involved in major transport functions, such as bumetanide, acetazolamide, and tetraethylammonium, may affect resting cell volume and volume regulation. Artifacts in water transport measurements using the *Xenopus oocyte* expression system have also led to the conclusion that a wide variety of drugs, including many common, chemically unrelated antiepileptics and carbonic anhydrase inhibitors, inhibit brain water channel aquaporin-4 (AQP4) (Huber et al., 2009), with
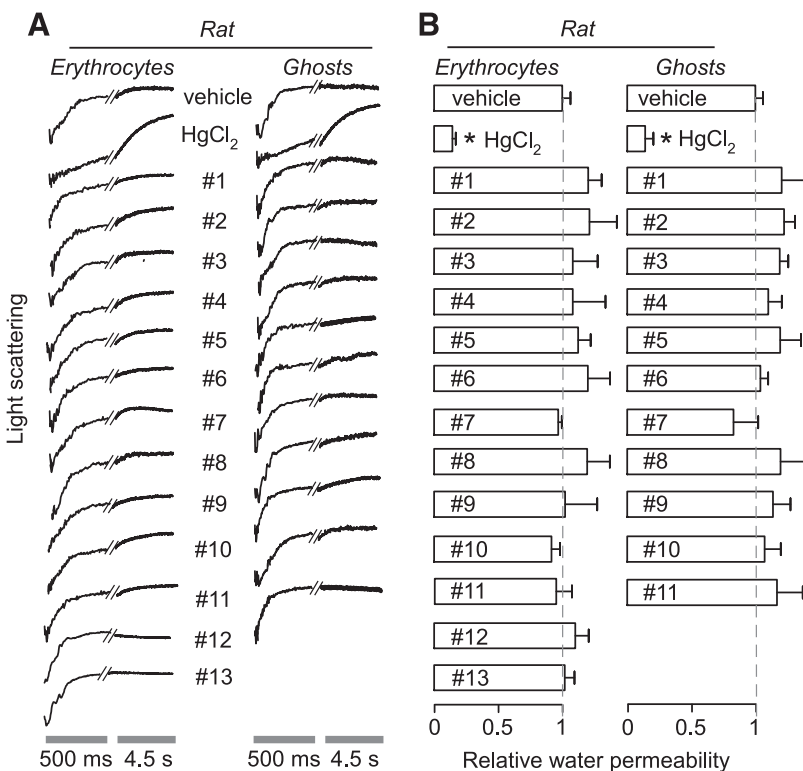
Fig. 6. Osmotic water permeability in rat erythrocytes and hemoglobin-free ghost membranes derived therefrom. Osmotic water permeability was measured from the time course of scattered light intensity in response to a 250 mM inwardly directed sucrose gradient. (A) Representative time course data for negative control (0.5% DMSO vehicle alone), 0.3 mM HgCl$_2$ (positive control), and indicated compounds (each 50 μM). Cells and ghosts were incubated with test compounds for ~15 minutes before measurements. (B) Relative osmotic water permeability (S.E., $n = 4$). *$P < 0.05$ compared with control.
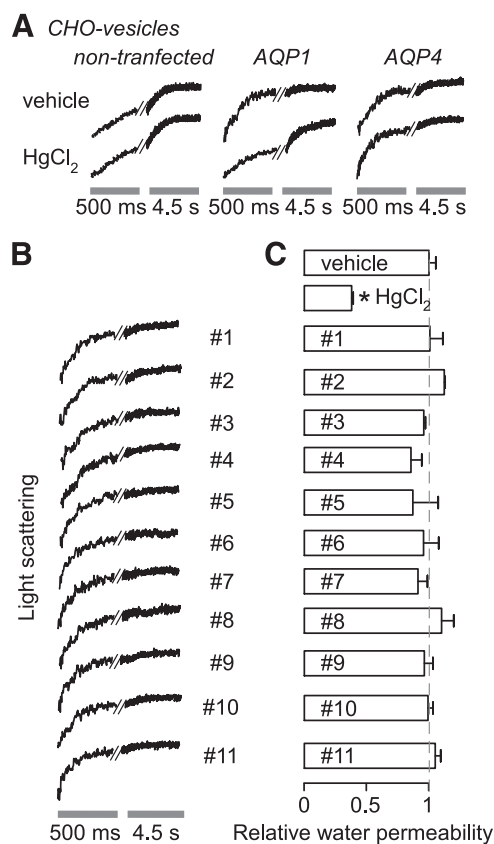
Fig. 7. Osmotic water permeability in plasma membrane vesicles from CHO cells. Osmotic water permeability was measured from the time course of scattered-light intensity in response to a 250 mM inwardly directed sucrose gradient. (A) Representative time course data for negative control (0.5% DMSO vehicle alone) and 0.3 mM HgCl₂ in vesicles from nontransfected CHO cells expressing AQP1- and AQP4-M23. (B) Representative time course data for indicated compounds (each 50 μM). Vesicles were incubated with test compounds for ~15 minutes before measurements. (C) Relative osmotic water permeability (S.E., $n = 4$). *$P < 0.05$ compared with control.

subsequent measurements failing to confirm inhibition (Yang et al., 2008). Given the apparent very low probability of identifying AQP inhibitors, it seems a priori unlikely that testing common drugs such as bumetanide, acetazolamide, antimigraines, and antiepileptics without large-scale screening would yield AQP inhibitors. It also seems unlikely that small molecules could activate AQP1, as its water permeability is constitutively high and not subject to regulation.

Compounds 1, 2, and 3 were identified by virtual (computational) screening of ~10⁶ compounds of the ZINC database and testing 14 compounds for inhibition of osmotic swelling in AQP1-expressing *Xenopus laevis* oocytes (Seeliger et al., 2013). The compounds were identified by molecular docking computations to a part of the extracellular surface of human AQP1. Compounds 1, 2, and 3 showed ~80% reduced osmotic swelling of the oocytes with an IC₅₀ of 8–20 μM. However, as found here, no inhibition was seen in light-scattering measurements on erythrocytes, suggesting an oocyte-specific action. A bona fide AQP1 inhibitor would be expected to produce inhibition in different assays and different cell systems.

Migliati et al. (2009) screened known channel blockers using the oocyte swelling assay. Although the identities and numbers of tested blockers were not mentioned, they focused on

loop diuretic inhibitors of the NKCC cotransporter, reporting inhibition by bumetanide. Of 45 bumetanide scaffolds synthesized, compound 4 here (AqB013) was identified in oocyte assays as an inhibitor of AQP1 and AQP4 with IC₅₀ ~20 μM. In a follow-on study by the same investigators, compound 4 was tested in a brain injury model for reducing edema, though no beneficial effect was found (Oliva et al., 2011). The same group later found that an analog of the loop diuretic furosemide, compound 5 here (AqF026), activated AQP1, increasing its water permeability by ~20% in the oocyte assay (Yool et al., 2013). The possibility that off-target actions of these compounds might be responsible for the apparent effects on oocyte water permeability, such as actions of the many NKCC-related ion transporters, was not considered.

Mola et al. (2009) screened approximately 3500 compounds using a calcein fluorescence assay in AQP1 and AQP4-expressing cells in a plate-reader assay in which cells were exposed to a 200 mM inwardly directed gradient of NaCl. Active compounds from the screen were retested using erythrocytes and vesicles derived from AQP4-expressing cells. Compounds 6, 7, 8, and 9 were reported to inhibit AQP1 with IC₅₀ values of 25–50 μM. In our hands these compounds showed marked toxicity at 100 μM (data not shown). Compounds 6, 7, and 8 are non-drug-like; compounds 6 and 8 are organolead and organotin molecules, respectively, which as a general class of molecules are considered to be neurotoxins (Chang, 1990) and cause erythrocyte lysis (Kleszcyńska et al., 1997). Compound 7 (trichopolyn I) is a structurally complex 10-residue lipopeptide isolated from the fungus *Trichoderma polysporum* that belongs to the trichogin class of lipopeptaibols antibiotics whose mechanism of action is thought to be pore formation in bacterial cell membranes (de Zotti et al., 2009).

Recently, To et al. (2015) reported two compounds, 10 (an analog of 9) and 11, as AQP1 inhibitors using a yeast freeze-thaw assay performed in *Escherichia coli* expressing AQP1, in which cell viability was measured after two-cycles of freeze-thaw. The stated, though nonvalidated, rationale is that AQP1 permits water efflux during thawing and prevents cell bursting. Their study included light-scattering measurements on erythrocytes, though interpretation of possible inhibitory effects was confounded by the multiexponential kinetics of the light-scattering data. Very recently, Patil et al. (2016) reported compounds 12 and 13 as AQP1 inhibitors in a small screen. Apparent compound activities were quite variable in *Xenopus* oocyte, erythrocyte ghost, and AQP1 proteoliposome assays. Here, we found both compounds to be toxic to erythrocytes and vesicles.

In conclusion, we could not demonstrate modulation of AQP1 function by 12 reported inhibitors and one reported activator using several direct assays of osmotic water permeability and different assay conditions. In view of the multiple potential clinical applications of AQP1 inhibitors, the identification of AQP1 inhibitors remains a high priority.